Exploration of BioMat-X

Open Exploration

Open Access Original Article

Direct observation of thermally induced fluctuation in lipid membranes using TEM-based gold nanoparticle tracking

Kazuhiro Mio[1,2,3†*], Takaaki Shiina[1,3†], Tatsunari Ohkubo[1,2,3], Tatsuya Arai[4,5], Daisuke Sasaki[4], Yuji C. Sasaki[1,4]

[1]AIST-UTokyo Advanced Operando-Measurement Technology Open Innovation Laboratory (OPERANDO-OIL), National Institute of Advanced Industrial Science and Technology (AIST), Chiba 277-0882, Japan

[2]Artificial Intelligence Research Center (AIRC), National Institute of Advanced Industrial Science and Technology (AIST), Tokyo 135-0064, Japan

[3]Graduate School of Medical Life Science, Yokohama City University, Yokohama 230-0045, Japan

[4]Graduate School of Frontier Sciences, The University of Tokyo, Chiba 277-8561, Japan

[5]Graduate School of Life Science, Hokkaido University, Sapporo 060-0810, Japan

[†]These authors contributed equally to this work.

***Correspondence:** Kazuhiro Mio, Artificial Intelligence Research Center (AIRC), National Institute of Advanced Industrial Science and Technology (AIST), 2-4-7 Aomi, Tokyo 135-0064, Japan. kazu.mio@aist.go.jp

Academic Editor: Laurent Muller, Collège de France, France

Received: December 4, 2025 **Accepted:** February 26, 2026 **Published:** March 4, 2026

Cite this article: Mio K, Shiina T, Ohkubo T, Arai T, Sasaki D, Sasaki YC. Direct observation of thermally induced fluctuation in lipid membranes using TEM-based gold nanoparticle tracking. Explor BioMat-X. 2026;3:101361. https://doi.org/10.37349/ebmx.2026.101361

Abstract

Aim: This study aims to develop and validate a transmission electron microscopy (TEM)–based approach for probing nanoscale lipid membrane dynamics by tracking the motion of gold nanoparticles dispersed on membrane surfaces.

Methods: Lipid thin films composed of dipalmitoylphosphatidylcholine (DPPC) or dioleoylphosphatidylcholine (DOPC) were prepared over 2 μm holes in Quantifoil grids, and 5 nm gold nanocolloids were introduced as tracer particles. Sequential TEM imaging was performed during controlled heating and cooling cycles, and nanoparticle trajectories were analyzed to obtain mean squared displacement (MSD) curves. These measurements enabled quantification of thermally driven membrane dynamics. The temperature dependent behavior was further compared with differential scanning calorimetry (DSC) of dehydrated lipid samples.

Results: DPPC exhibited a pronounced MSD peak near 52.5 °C during the first heating cycle, corresponding to its main phase transition, whereas DOPC showed gradual and continuous mobility changes consistent with its intrinsically disordered acyl chains. Differences between electron beam molecular dynamics (EBMD) and DSC transition temperatures likely arose from dehydration and thin film geometry. Across repeated thermal cycles, DPPC membranes displayed cycle dependent changes in MSD profiles, suggesting annealing induced homogenization and potential beam induced structural alterations.

Conclusions: EBMD provides real space, time resolved visualization of nanoscale membrane fluctuations and complements ensemble techniques such as DSC, fluorescence recovery after photobleaching (FRAP),

and nuclear magnetic resonance (NMR). The TEM based particle tracking approach reliably distinguishes ordered versus disordered lipid systems and offers a versatile platform for investigating soft biological membranes, including systems containing proteins or heterogeneous lipid compositions.

Keywords

membrane dynamics, transmission electron microscopy, nanoparticle tracking, electron beam molecular dynamics, phase transition, phospholipids

Introduction

Understanding molecular dynamics is fundamental to elucidating structure–function relationships in various materials [1]. Lipid bilayers, as the essential structural framework of biological membranes, play central roles in cellular signaling, transport, and compartmentalization. Their dynamic behavior, including phase transitions and molecular mobility, is closely linked to their physicochemical properties such as lipid composition, temperature, and hydration, and is directly associated with membrane function.

Various analytical techniques have been developed to investigate lipid dynamics, including fluorescence recovery after photobleaching (FRAP), nuclear magnetic resonance (NMR), and differential scanning calorimetry (DSC) [2–4]. These methods have provided valuable insights into lipid phase behavior and diffusion; however, they largely rely on indirect indicators or ensemble measurements, which may obscure local heterogeneities and transient dynamic phenomena.

In parallel, our group has developed X-ray-based time-resolved motion analysis techniques, such as diffracted X-ray tracking (DXT) and diffracted X-ray blinking (DXB) [5–7]. These approaches capture molecular motions with nanosecond and picometer resolution, enabling detailed characterization of diverse biomolecules and materials under adjustable experimental conditions [8–12]. More recently, we have successfully applied the core principles of these methods to transmission electron microscopy (TEM) analysis. By dispersing gold nanoparticles onto material surfaces and tracking their motion with TEM, we established an electron beam molecular dynamics (EBMD) approach capable of visualizing the nanoscale dynamics of synthetic polymers [13]. This prior work confirmed that EBMD can sensitively distinguish molecular characteristics of relatively stable polymers.

In the present study, we extend EBMD to biologically relevant lipid membranes, focusing on dipalmitoylphosphatidylcholine (DPPC) and dioleoylphosphatidylcholine (DOPC), two representative saturated and unsaturated phospholipids, respectively. Unlike synthetic polymers, lipid molecules undergo well-defined thermal phase transitions and are more susceptible to electron-beam damage, providing both a challenge and an opportunity to assess the applicability of EBMD in more fragile and heterogeneous systems.

By tracking gold nanoparticles on DPPC and DOPC membranes during controlled heating and cooling cycles, we assessed both the feasibility and limitations of EBMD in fragile biological systems. Beyond validating this methodology, the present work highlights EBMD as a potential platform for probing nanoscale membrane biophysics with high spatial and temporal resolution, providing a complementary perspective to established ensemble-based techniques.

Materials and methods

Preparation of TEM samples

DPPC (Sigma-Aldrich, Inc., St. Louis, MO, USA) and DOPC (Tokyo Chemical Industry Co., Ltd., Tokyo, Japan) were dissolved in chloroform at concentrations of 5 mg/mL. A 5 nm gold nanocolloid solution (BBI Solutions, Crumlin, UK) was sonicated for 10 min in a Branson M1800-J Ultrasonic Bath (Branson Ultrasonics, Brookfield, CT, USA). A 5 μL aliquot of the lipid solution was applied to a Quantifoil Cu #200 R2/2 grid (Quantifoil Micro Tools GmbH, Großlöbichau, Germany) and air-dried. Subsequently, 2 μL of the

dispersed gold nanocolloid solution was applied, incubated for 3 min, blotted with filter paper, and air-dried at room temperature.

TEM observation

TEM observation was performed using a JEM-1230 (JEOL Ltd., Tokyo, Japan) operated at 100 kV with a magnification of 40,000×. The current density during imaging was maintained at 1–10 pA/cm^2. Images were acquired with a FastScan-F114 CCD camera (TVIPS GmbH, Gauting, Germany; 1,024 × 1,024 pixels, 14 × 14 μm^2 pixel size) controlled by EM-MENU software (TVIPS GmbH). Real-time TEM videos were recorded at 12 fps using OBS Studio (Open Broadcaster Software, OBS Project, https://obsproject.com) by capturing the EM-MENU display window.

Temperature control was achieved with a Peltier heating/cooling sample holder (KITANO SEIKI Co., Ltd., Tokyo, Japan) under PID regulation, maintaining temperature change rates ≤ 0.1°C/s. The holder allowed specimen temperatures between –30°C and 100°C. For video recording of DPPC dynamics, grids were first cooled from room temperature to 0°C, then heated stepwise to 98°C, followed by cooled back to 0°C. This heating–cooling cycle was repeated three times. For DOPC, specimens were first cooled from room temperature to –26°C, then heated to 60°C, followed by cooled again to –26°C. The experimental temperature ranges were selected based on reported phase transition points for DPPC and DOPC [14–18].

Mean squared displacement and probability density analysis

Video files were converted into continuous image sequences using FFmpeg (https://ffmpeg.org). Each frame was processed using ImageJ (Rasband, W.S., U.S. National Institutes of Health, Bethesda, MD, USA; https://imagej.net/ij/) for background correction, black/white inversion, and brightness and contrast adjustment to optimize particle identification.

Particle identification and mean squared displacement (MSD) calculation were performed using TrackPy (v0.3.2, https://doi.org/10.5281/zenodo.60550). Individual gold nanoparticles were detected in each frame and linked across consecutive frames using the link_df() function, which associates particle positions based on a maximum allowed displacement between frames, enabling simultaneous tracking of multiple particles while preserving unique trajectories. The MSD curves were further analyzed using custom routines implemented in IGOR Pro version 9 (Wavemetrics, Lake Oswego, OR, USA). Near the transition temperatures, nanoparticle motion increased, and some particles moved out of the field of view or exhibited reduced contrast, resulting in lower numbers of valid displacement events (n) compared with other temperature regions. The effective pixel size was calibrated based on the apparent diameter of the gold nanoparticles measured in ImageJ, yielding a pixel size of 0.392 nm.

Probability density (PD) analysis was conducted at a fixed lag time of Δt = 8 s. This lag time was selected based on a previous study in which MSD values were evaluated at one-second intervals from Δt = 1 s to Δt = 9 s, identifying Δt = 8 s as an appropriate timescale for comparing temperature-dependent differences and reported material properties [13]. Each experiment corresponds to a measurement at a single, fixed temperature. For each experiment, 121 frames were recorded at a frame rate of 12 frames per second, corresponding to a total acquisition time of 10 s. From each trajectory, 25 non-overlapping displacements corresponding to Δt = 8 s were extracted to avoid correlation between successive measurements. Displacements from all tracked particles were pooled to construct a single PD histogram for each experiment. Accordingly, the reported values (e.g., 2,784–7,171 for DPPC and 125–267 for DOPC) represent the total number of individual displacement events accumulated over all particles, rather than the number of particles.

The PD histograms of nanoparticle displacements at Δt = 8 s were plotted and fitted with single or multiple Gaussian functions using IGOR Pro to describe the distribution of nanoparticle motion. When multiple Gaussian components were required, this was interpreted as the coexistence of distinct mobility populations near the phase transition. Box plots were generated directly from the pooled displacement data (Δr), where the box boundaries represent the 25th and 75th percentiles, the central line indicates the median, and the whiskers denote the minimum and maximum values.

Differential scanning calorimetry

Samples inside the electron microscope are effectively dehydrated due to the high-vacuum environment. To compare dynamics under similar conditions, DSC measurements were performed on fully dehydrated samples. DPPC and DOPC samples were dehydrated at 80°C for 18 h under vacuum (CVE-2100, TOKYO RIKAKIKAI CO., LTD., Tokyo, Japan). Dehydrated DPPC (4.0 mg) and DOPC (12.2 mg) were sealed in 25 μL aluminum pans with lids, and DSC measurements were carried out using a DSC 3 instrument (Mettler Toledo International Inc., Greifensee, Switzerland). Thermal cycles were conducted from 0°C to 100°C for DPPC and from –80°C to 60°C for DOPC at a heating/cooling rate of 5°C/min under a nitrogen atmosphere. Each heating–cooling cycle was repeated multiple times to ensure reproducibility.

Results

In our previous study, we employed an EBMD approach to investigate synthetic polymers, successfully distinguishing the molecular characteristics of synthetic polymers PC_8FA (poly{2-(perfluorooctyl)ethyl acrylate}) and PSA (poly(stearyl acrylate)) [13]. In the present study, we applied this method to biologically relevant molecules (lipids) to further demonstrate its versatility.

Lipid membrane dynamics via EBMD

EBMD was applied to biologically relevant lipid membranes to assess its versatility beyond synthetic polymers, previously studied for PC_8FA (poly{2-(perfluorooctyl)ethyl acrylate}) and PSA (poly(stearyl acrylate)) [13]. Because TEM observations were conducted under high vacuum, the lipid membranes were effectively dehydrated. This dehydration is known to shift the main phase transition temperature (Tm) of DPPC from approximately 41°C in fully hydrated bilayers to 50–75°C or higher in dehydrated states [14, 15]. To account for this effect, DSC measurements were also performed on dehydrated samples for direct comparison with EBMD results. Lipid films of DPPC and DOPC, dissolved in chloroform, were deposited onto Quantifoil Cu #200 R2/2 grids with 2-μm–diameter holes. 5-nm gold nanoparticles were dispersed on the films as tracer probes. Both DPPC and DOPC formed stable membranes spanning the holes, similar to previously reported polymer systems [13]. Representative TEM images show continuous lipid membranes spanning the Quantifoil holes (Figure 1c, Figure S1). These observations confirm that the membranes indeed extend across unsupported regions rather than adhering solely to the carbon film. However, the membrane thickness and lamellarity cannot be strictly determined from conventional TEM contrast alone, and single-bilayer formation cannot be unequivocally concluded. Membrane dynamics were recorded using a Peltier-type heating/cooling TEM holder (KITANO SEIKI Co., Ltd., Tokyo, Japan), which allows precise temperature control from −30°C to 100°C. Video recordings were captured in a conventional JEOL1230 electron microscope during heating and cooling cycles, and MSD of gold nanoparticles was calculated at each temperature point to quantify membrane dynamics (Figure 1a–e). Representative raw EBMD image movies recorded at different temperatures are provided (Movies S1–S6).

DPPC contains two saturated 16-carbon chains (palmitic acid, C16:0), whereas DOPC contains two monounsaturated 18-carbon chains (oleic acid, C18:1 cis-Δ9) (Figure 1f). Despite their structural similarity, these lipids exhibit markedly different membrane properties due to the presence or absence of unsaturated acyl chains. We examined their main phase transition temperatures (melting temperatures: Tm) and crystallization temperatures (Tc) using a DSC. It is well established that the transition temperature of phospholipids largely depends on hydration state [14–18]. Because samples inside the electron microscope are effectively dehydrated under high vacuum, DSC measurements were conducted on dehydrated specimens for direct comparison. DSC demonstrated a Tm and Tc of dehydrated DPPC were 64°C and 62°C, respectively, while 3°C and −20°C for dehydrated DOPC (Figure 1g, 1h). These values confirm low hydration conditions of the specimens used in our experiments (Figure S4). In this experiment, DSC experiments were performed at a heating/cooling rate of 5°C/min under a nitrogen atmosphere. Although slower DSC scan rates may yield sharper transition features, the aim of the present DSC measurements was to identify approximate phase transition temperatures rather than to perform a detailed thermodynamic analysis. As the reproducibility of the observed transitions and their consistency with reported values (approximately

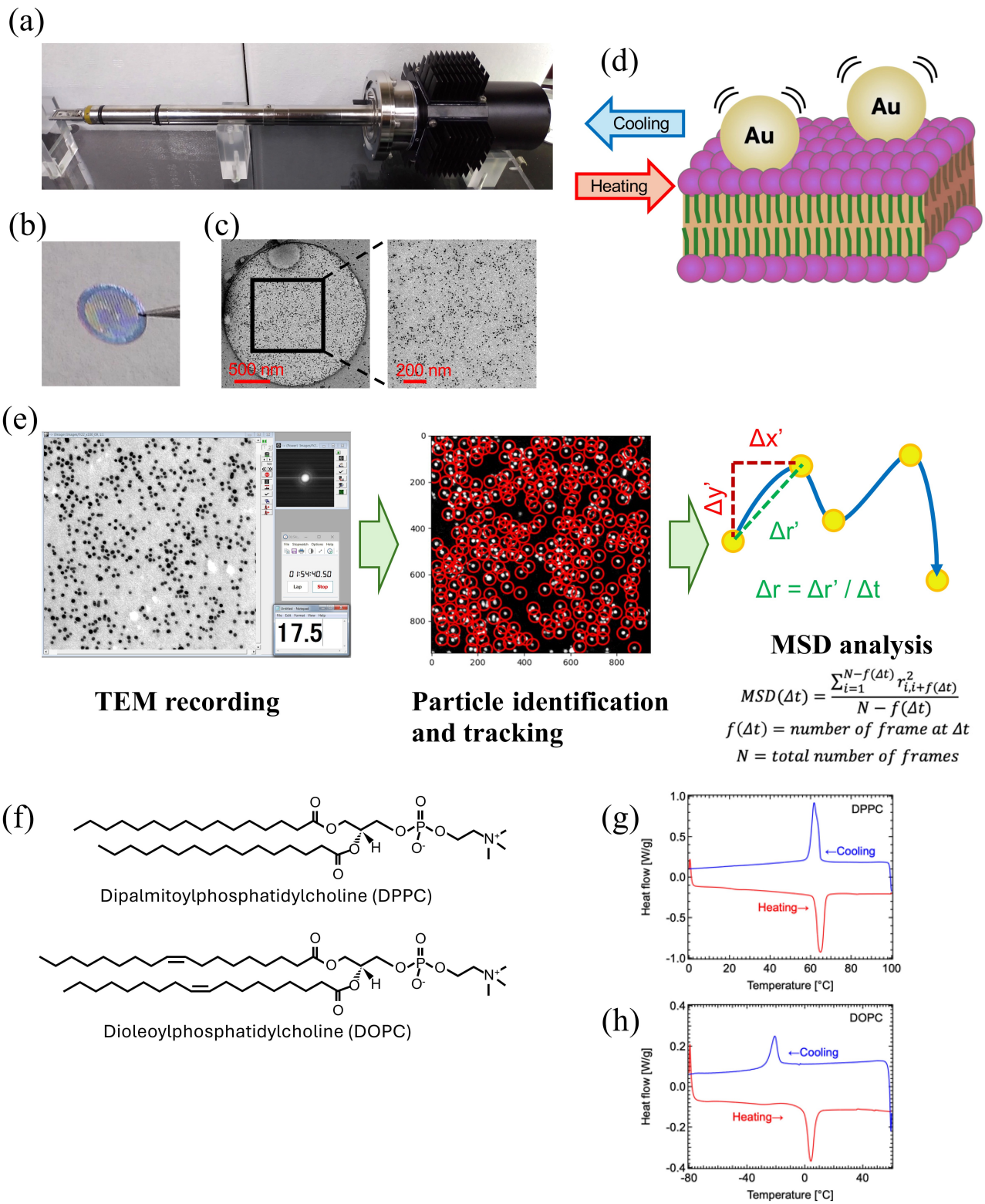

Figure 1. Experimental procedure and lipid membrane preparation. (**a**) Peltier-based heating/cooling TEM holder (KITANO SEIKI, Tokyo, Japan), enabling temperature control from –30°C to +100°C. (**b**) Lipid thin films formed across the holes of a Quantifoil Cu #200 R2/2 grid. (**c**) Representative TEM image of colloidal gold particles adsorbed on a DPPC membrane. (**d**) Magnified view of gold nanoparticles embedded on the lipid surface. (**e**) Flowchart of the data analysis process. Gold nanoparticles were used to observe thermal-induced phospholipid fluctuation using the electron microscopy. MSD of the gold nanoparticle movement was analyzed from the video data. (**f**) Chemical structures of DPPC (saturated) and DOPC (unsaturated). (**g**) Differential scanning calorimetry (DSC) thermograms of DPPC (dehydrated form) and (**h**) DOPC (dehydrated form), demonstrating their respective thermal transition behaviors.

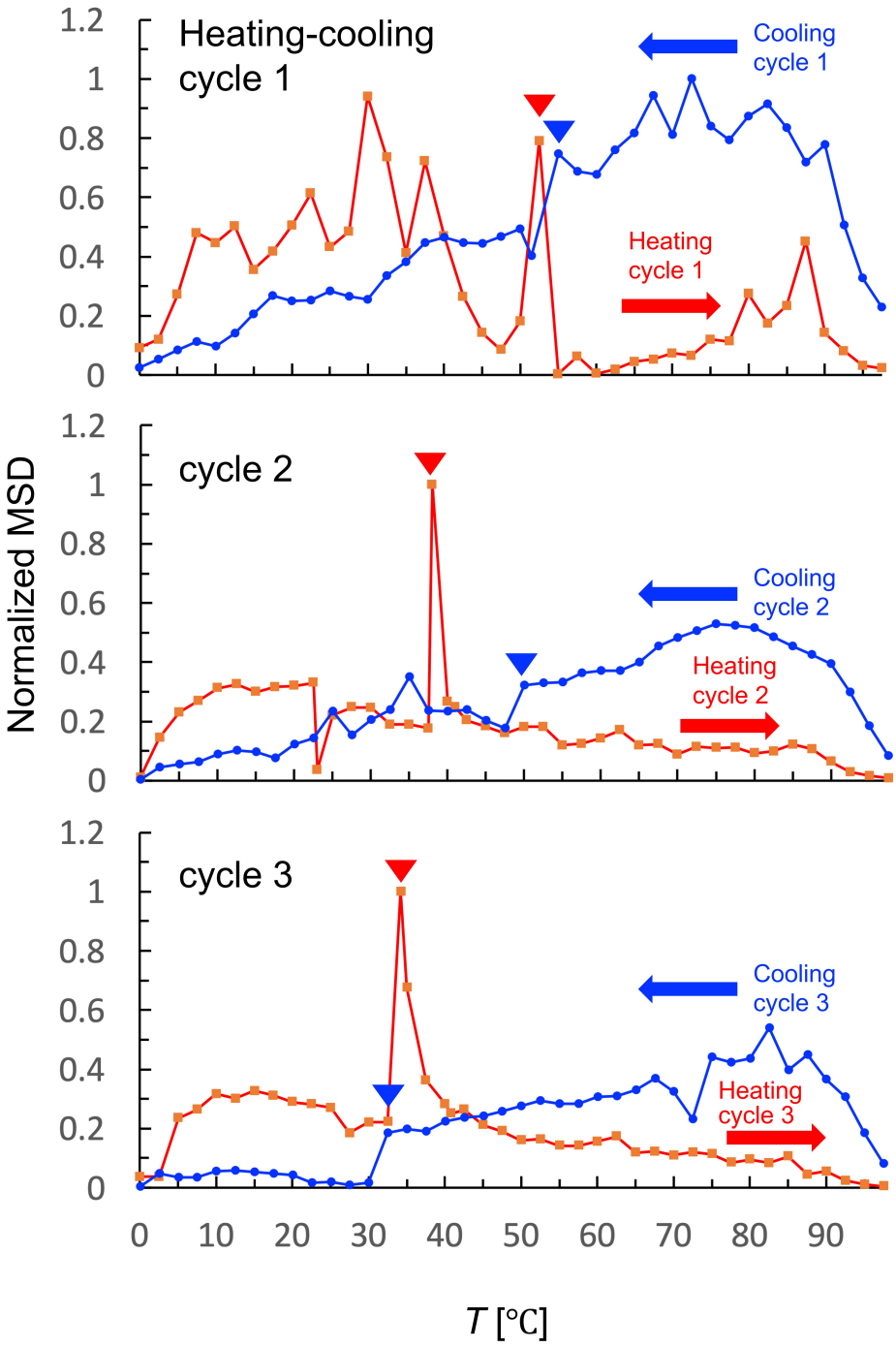

Figure 2. Temperature-dependent dynamics of DPPC membranes during repetitive thermal cycling. Normalized MSD of gold nanoparticles tracked on DPPC membranes during three repetitive heating and cooling cycles (0–98°C). MSD values were calculated at Δt = 8 s and normalized to the maximum value. Red and blue arrowheads indicate the phase-transition temperatures manually identified from the EBMD data.

41°C in fully hydrated bilayers to 50–75°C or higher), a scan rate of 5°C/min was considered sufficient for defining the temperature window relevant to the EBMD experiments (Figure S4).

EBMD observation of DPPC membrane fluctuation

To evaluate the temperature-dependent dynamic of DPPC, MSD measurements using EBMD were repeated three times over a heating–cooling cycle (0–98°C) by maintaining temperature change rates ≤ 0.1°C/s (Figure 2, Figure S5). The normalized MSD curves for the heating-cooling cycles are shown (Figure 2). In the first heating cycle, multiple MSD fluctuations were observed between 6°C and 40°C, and a prominent MSD peak appeared around 52.5°C, corresponding to phase-transition-related fluctuations. The discrepancy in Tm observed between EBMD and DSC, which was also noted in our previous polymer

analysis [13], likely arises from EBMD's sensitivity to local, non-equilibrium molecular dynamics preceding the bulk phase transition, as well as differences in sample environment, including thin-film geometry and partial hydration. Low-temperature fluctuations between 6°C and 40°C may reflect heterogeneity in membrane domains or residual hysteresis from sample preparation.

Analyses using FRAP and NMR have reported that above the transition temperature (Tm), molecular mobility increases markedly, with diffusion constants rising by one to two orders of magnitude [19, 20]. In contrast, our TEM-based MSD analysis did not show a pronounced change, possibly due to differences in detection sensitivity or the motion tracking index, here represented by gold nanoparticle movement. It should be noted that the MSD of the gold nanoparticles does not directly correspond to the lateral diffusion coefficient of individual lipid molecules. Because each particle is coupled to multiple lipids, the measured Δr reflects the effective, collective mobility of the membrane over nanometer length scales, which is sensitive to membrane heterogeneity, viscoelasticity, and domain formation.

When comparing the results of successive heating cycles, the MSD profiles changed markedly. Low-temperature peaks disappeared in the first and second heating cycles, while a dominant peak appeared around 38°C in the second cycle and shifted to 34°C in the third cycle. These changes suggest that initially heterogeneous DPPC domains became more homogeneous multilamellar after thermal annealing, as reported in previous papers [21, 22]. However, the progressive downward shift in transition temperatures across cycles may reflect potential electron-beam damage or structural destabilization [23, 24]. Despite the annealing effect, large gaps in the MSD curves were observed between 22.5–30°C in the second cycle and 25–30°C in the third cycle, which may correspond to the "pretransition shift" of DPPC from the Lamellar tilted gel phase (Lβ′) to the Ripple gel phase (Pβ′) [25]. To evaluate the possibility that lipid films preferentially adhere to the carbon support, as reported for aqueous lipid samples [26], we examined the carbon–hole boundaries in our preparations. TEM images show that gold nanoparticles are present on both carbon and hole regions, suggesting that organic-solvent deposition distributes lipids across both areas, although some aggregation near carbon edges is observed (Figure S1).

In the cooling cycles, MSD remained relatively high at higher temperatures but declined sharply near 54°C in the first cycle, corresponding to membrane recrystallization (Figure 2). At temperature below Tc, the MSD levels were significantly reduced compared to pre-transition values. Fluctuations diminished across repeated cooling cycles, supporting the idea that initial heterogeneity was resolved by thermal annealing. The sharp MSD decline observed at 54°C in the first cycle shifted to 50°C in the second cycle and 32°C in the third cycle, likely reflecting cumulative electron-beam damage again. Based on these observations, subsequent analyses focused primarily on the first heating–cooling cycle, where the original membrane structure was best preserved.

Dynamics around phase transition temperature (DPPC)

Molecular dynamics of the DPPC membrane near Tm and Tc were analyzed in detail (Figures 3 and 4). Just below Tm in the heating cycle 1, motion histograms showed broad distributions fitted by multiple Gaussian components (Figure 3b), indicating coexistence of distinct molecular motion modes, likely due to structural heterogeneity or fabrication-induced hysteresis. At 52.5°C, both overall mobility and histogram complexity increased, requiring four Gaussian components for fitting. After exceeding Tm, dynamics became more uniform, with a single Gaussian adequately describing the distribution, reflecting a homogeneous membrane.

During cooling, no major fluctuations were observed aside from a ~10% drop in mobility between 54°C and 52°C (Figure 4a). Histogram distributions before and after Tc indicated that recrystallization proceeded relatively uniformly, transitioning from two Gaussian components to one (Figure 4b).

EBMD observation of DOPC membrane fluctuation

To further validate the versatility of EBMD, DOPC was examined. Although DOPC shares the same headgroup as DPPC, its unsaturated acyl chains confer distinct physical properties (Figure 5). DSC measurements of dehydrated DOPC confirmed a Tm of 3°C and a Tc of −20°C (Figure 1h).

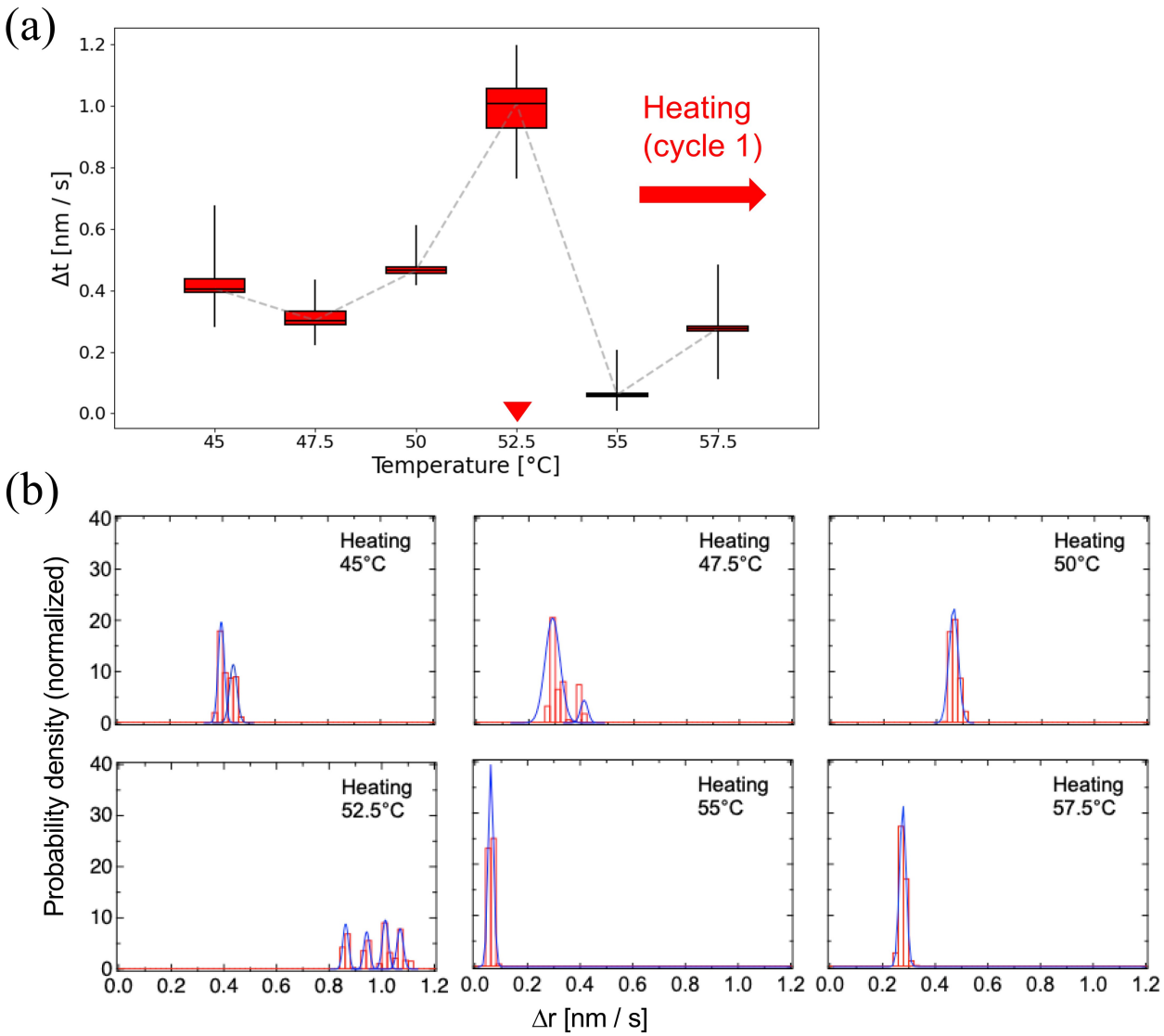

Figure 3. Molecular dynamics of DPPC membranes near the main phase transition during the first heating cycle. (**a**) Box plot representation of nanoparticle motion between 45–57.5°C. The box plots indicate the minimum, 25th percentile, median, 75th percentile, and maximum values. Red arrowhead indicates the phase-transition temperatures manually identified from the EBMD data. The original box plots spanning the wide-range temperature are shown in Figure S2a. (**b**) Probability density histograms of particle displacements at selected temperatures near 52.5°C. The histograms were fitted with single or multiple Gaussian curves to reveal the coexistence of heterogeneous motion modes.

In contrast to DPPC, DOPC exhibited no distinct peaks in the MSD profile during either the heating (Figure 5a) or cooling (Figure 5b) cycles. The cis double bond–induced disorder in DOPC may disrupt tight molecular packing and prevent sharp phase transitions. During heating, membrane mobility gradually increased up to −10°C and plateaued near Tm (3°C), followed by irregular fluctuations indicative of dynamic disorder rather than discrete phase transitions (Figure 5a). Motion histograms showed minimal changes around Tm with slight variation after the transition (Figure 5c). During cooling, mobility decreased continuously, with a marked reduction below −20°C, consistent with Tc, and histogram distributions remained largely unchanged (Figure 5b, 5d).

Discussion

Recently, TEM has emerged as a powerful tool for nanoscale imaging, and its application has expanded to the study of soft and dynamic materials [27–32]. In this context, the present study demonstrates the applicability of EBMD to lipid membranes, extending our previous work on synthetic polymers to more fragile biological molecules. By tracking gold nanoparticles dispersed on DPPC and DOPC films, we directly visualized thermally induced membrane dynamics and identified distinct behaviors between saturated and unsaturated phospholipids.

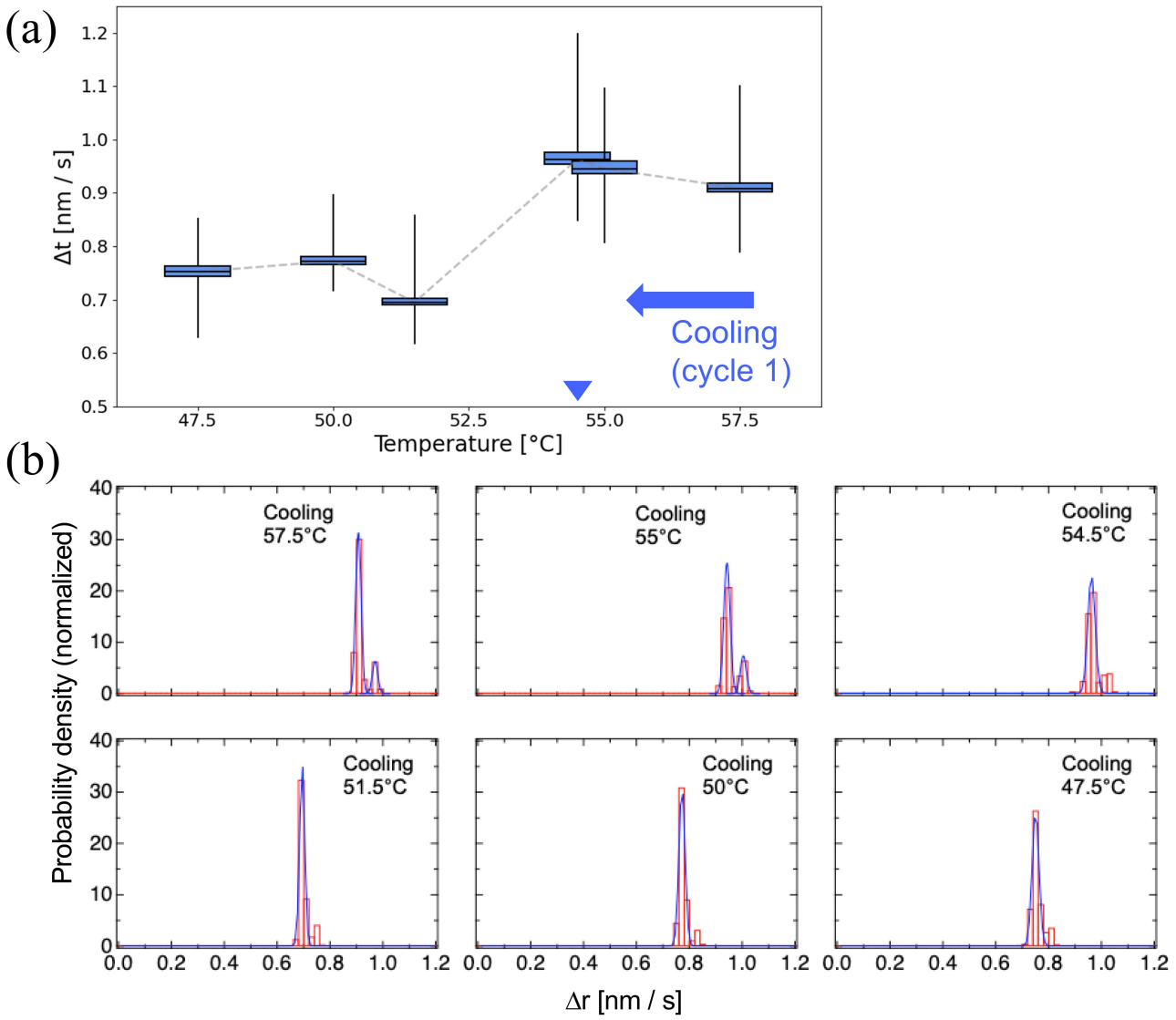

Figure 4. Molecular dynamics of DPPC membranes during the first cooling cycle. (**a**) Box plot representation of nanoparticle motion between 47.5–57.5°C. Blue arrowhead indicates the phase-transition temperatures manually identified from the EBMD data. The original box plots spanning the wide-range temperature are shown in Figure S2b. (**b**) Probability density histograms of particle displacements at selected temperatures near the recrystallization point (~54.5°C). Gaussian fitting was applied to each histogram.

Compared with established approaches, EBMD provides a complementary perspective to ensemble-based techniques. DSC accurately measures thermodynamic phase transition processes in lipid components and can capture sample heterogeneity, for example through broadened or multi-component transitions. In contrast, EBMD tracks the motion of tracer nanoparticles in real space, enabling direct visualization of local and transient membrane dynamics at the nanoscale that are averaged out in bulk calorimetric measurements.

Other techniques also have inherent limitations. Fluorescence-based methods, such as FRAP or DPH anisotropy (1,6-diphenyl-1,3,5-hexatriene fluorescence anisotropy) probe membrane fluidity but rely on exogenous labels and report averaged bulk behavior. NMR spectroscopy provides information on acyl-chain order and diffusion, yet lacks the spatial resolution required to capture local and transient events. In contrast, EBMD provides real-space, time-resolved trajectories of tracer particles adsorbed on the membrane surface, offering an indirect, tracer-based readout of effective membrane dynamics at the nanoscale. While this approach does not directly measure intrinsic lipid molecular fluctuations, it sensitively reports on collective membrane motions and local variations in effective mobility, which may reflect underlying heterogeneity in membrane organization.

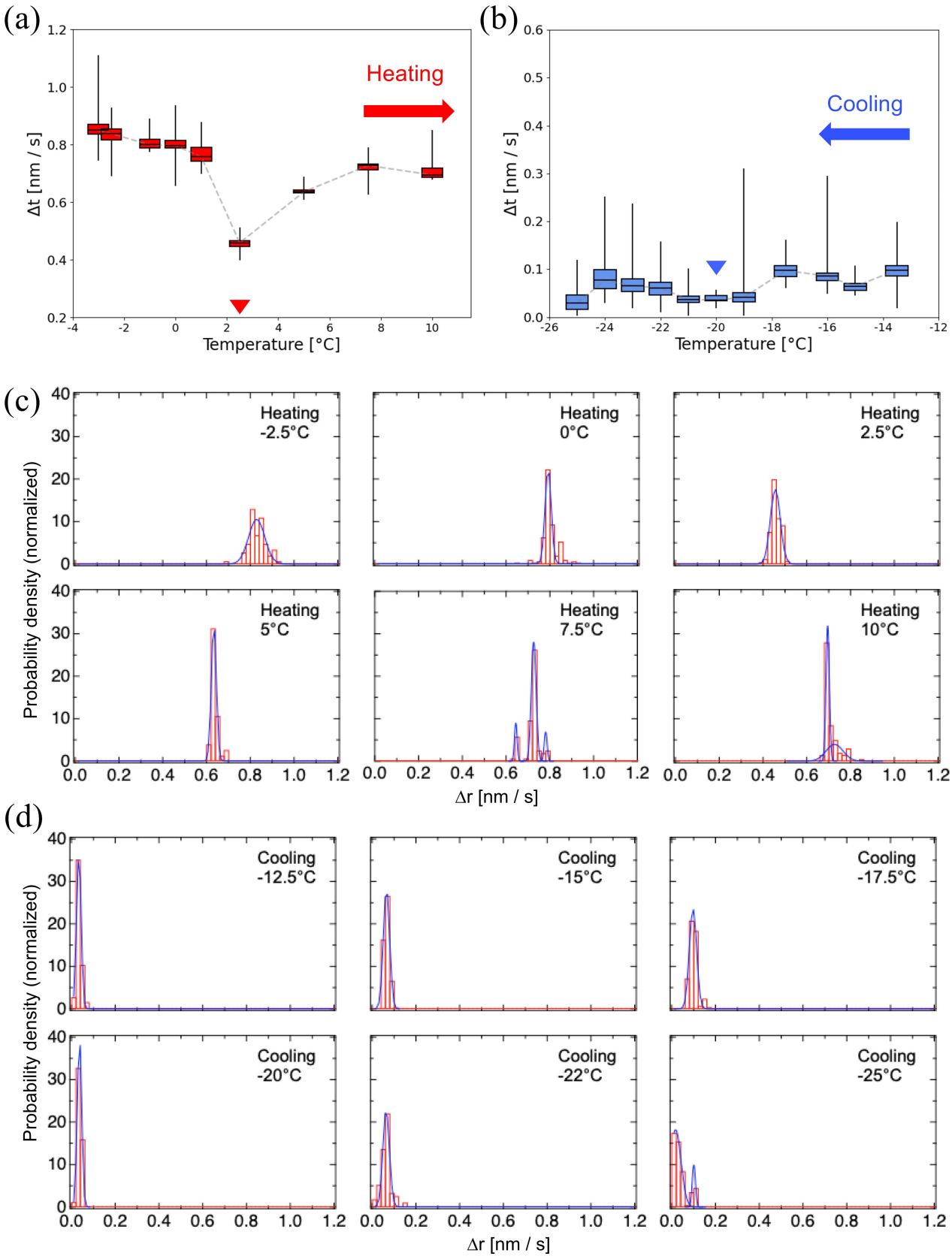

Figure 5. Temperature-dependent dynamics of DOPC membranes. Box plots of nanoparticle motion recorded between –25°C and 25°C during (**a**) heating and (**b**) cooling cycles. Red and blue arrowheads indicate the phase-transition temperatures manually identified from the EBMD data. The original box plots spanning the wide-range temperature are shown in Figure S3a and Figure S3b. Probability density histograms of particle displacements (**c**) near the main transition (3°C) and (**d**) crystallization (–20°C) temperatures, respectively. Histograms were fitted by Gaussian functions.

Beyond simple thermal shifts, EBMD revealed behaviors not readily resolved by ensemble-averaging techniques. In DPPC membranes, heterogeneous fluctuations persisted below the main transition temperature, consistent with metastable states or domain structures that progressively annealed during repeated heating cycles. By contrast, DOPC membranes exhibited no discrete transition but displayed irregular, disordered fluctuations over a broad temperature range, reflecting the fluidizing effect of cis double bonds. These observations highlight the ability of EBMD to capture local and transient dynamics that are obscured in bulk measurements.

Lipid phase transition temperatures are strongly influenced by hydration state and structural constraints. Fully hydrated multilamellar DPPC exhibits a sharp main transition at approximately 41°C [17] (Figure S4), whereas dehydration shifts this transition to higher temperatures: Partially hydrated or powdered DPPC melts between 50 and 75°C, and fully anhydrous samples can approach 100°C [18]. Consistent with these effects, our DSC measurements showed transition temperatures of 52.5°C for DPPC and 3°C for DOPC in dehydrated TEM samples constrained in thin films.

Although fully hydrated membranes represent physiological conditions, dehydrated lipid states are also biologically relevant in several systems. For example, cryptobiotic organisms such as *Polypedilum vanderplanki* larvae and tardigrades can survive near-complete desiccation, in which the phase behavior of anhydrous lipid membranes is thought to contribute to structural stability in concert with protective molecules such as trehalose and specific proteins [33, 34]. Similarly, dehydrated lipid phase transitions play critical roles in plant seeds and pollen, where reversible phase changes during drying and rehydration are essential for long-term viability [35]. These examples highlight that membrane dynamics under low-hydration conditions, as probed here by EBMD, provide biologically meaningful insights into systems in which dehydration is central to survival or preservation, even though such conditions differ from those of fully hydrated cellular membranes.

The physical state of the samples also differed between measurement platforms. In the EBMD experiments, the lipids are considered to exist as multilayer assemblies rather than as single bilayers, forming heterogeneous stacks that included lamellar and blister-like structures [36, 37]. This interpretation is based on previous reports describing multilayer formation during organic-solvent deposition and on qualitative thickness observations; it should therefore be regarded as a working hypothesis rather than a definitive structural assignment. Accordingly, the apparent discrepancies between EBMD and DSC results—also observed in our previous work on synthetic polymers [13]—likely reflect differences in sample environments and structural organization.

Several additional limitations should be considered. Biological materials, consisting mainly of light elements, are highly sensitive to electron-beam damage, even at the lowest usable dose [23, 24]. Some degree of structural alteration is likely to occur during the initial scan. Indeed, the apparent transition temperatures tended to decrease during repeated cycles.

This susceptibility is likely enhanced in phospholipids such as DPPC and DOPC, which contain radiation-sensitive ester and phosphate ester linkages and, in the case of DOPC, unsaturated bonds, and lack the robust covalent backbones (e.g., C–C or C–F bonds) that confer higher radiation tolerance to synthetic polymers such as PSA and PC_8FA [13]. Further dose reduction may be necessary.

The use of gold nanoparticles as tracers represents another source of uncertainty. Although the MSD curves reflect nanoparticle motion rather than the intrinsic molecular dynamics of the lipid matrix, our previous polymer study showed pronounced MSD transitions at approximately 85°C for PC_8FA and 57.5°C for PSA [13]. In the present study, analogous transitions were observed at around 52.5°C for DPPC and 2.5°C for DOPC. This correspondence across chemically distinct systems supports the interpretation that the observed MSD variations primarily reflect temperature-dependent membrane dynamics rather than nanoparticle redistribution. Nevertheless, nanoparticle–lipid interactions may still influence local behavior. Because the measured dynamics originate from gold nanoparticle motion, it is possible that the nanoparticles report the behavior of a locally perturbed lipid environment rather than that of bulk lipids. If nanoparticles are partially embedded in the lipid layer, their presence may disturb local lipid packing and

elasticity and bias the measured mobility. In addition, changes observed between repeated heating–cooling cycles could, in principle, arise from temperature-dependent reorganization or redistribution of nanoparticles within the membrane. Although no clear evidence for systematic nanoparticle clustering or segregation was observed, such contributions cannot be fully excluded and should be considered when interpreting cycle-dependent EBMD results. In addition, hydration control remains critical. Correlating EBMD results with precisely defined water contents will be essential for quantitative comparison with DSC and other calorimetric methods. Lipid concentration and membrane thickness were also not strictly controlled in the present experiments, and systematic optimization of deposition conditions will be required in future studies.

Despite these limitations, EBMD has considerable potential for investigating more complex and biologically relevant membrane systems. Using advanced high-end electron microscopes equipped with direct electron detection cameras and photon-counting technology may allow us to further reduce electron dose and improve data reliability. Techniques such as liquid-cell TEM may allow observations under more native, hydrated conditions while reducing tracer-related artifacts. Observation of cholesterol-containing bilayers, which exhibit coexisting ordered and disordered domains, represents a natural next target for real-space dynamic tracking. Similarly, membranes incorporating proteins such as ion channels or viral fusion proteins could be examined to directly assess the interplay between phase behavior and functional conformational dynamics. In this way, EBMD complements established ensemble-based techniques by providing a nanoscale, real-space window into membrane biophysics and establishes electron microscopy as a versatile tool for studying both artificial and biological soft materials.

Abbreviations

DOPC: dioleoylphosphatidylcholine

DPPC: dipalmitoylphosphatidylcholine

DSC: differential scanning calorimetry

EBMD: electron beam molecular dynamics

FRAP: fluorescence recovery after photobleaching

MSD: mean squared displacement

NMR: nuclear magnetic resonance

PD: probability density

TEM: transmission electron microscopy

Supplementary materials

The supplementary figures for this article are available at: https://www.explorationpub.com/uploads/Article/file/101361_sup_1.pdf. The supplementary movies for this article are available at: https://www.explorationpub.com/uploads/Article/file/101361_sup_2.pdf.

Declarations

Acknowledgments

We thank Kayoko Kawaguchi and Mayui Sugiura at the National Institute of Advanced Industrial Science and Technology (AIST) for their daily assistance with the experiments.

Author contributions

KM: Writing—original draft, Investigation, Visualization, Supervision, Conceptualization. TS: Writing—review & editing, Investigation, Formal analysis. TO: Writing—review & editing. TA: Writing—review & editing. DS: Writing—review & editing. YCS: Writing—review & editing, Investigation, Supervision, Conceptualization. All authors read and approved the submitted version.

Conflicts of interest

The authors declare that there are no conflicts of interest.

Ethical approval

Not applicable.

Consent to participate

Not applicable.

Consent to publication

Not applicable.

Availability of data and materials

The raw data supporting the conclusions of this manuscript will be made available by the authors, without undue reservation, to any qualified researcher.

Funding

This work was supported by JSPS KAKENHI Grant Numbers [JP 23K26511, JP 23H01818, JP 24K09763, JP 21K06515, Japan], JST CREST grant number [JP18071859, Japan]. The funders had no role in study design, data collection and analysis, decision to publish, or preparation of the manuscript.

Publisher's note

References

1. Ohkubo T, Shiina T, Kawaguchi K, Sasaki D, Inamasu R, Yang Y, et al. Visualizing Intramolecular Dynamics of Membrane Proteins. Int J Mol Sci. 2022;23:14539. [DOI] [PubMed] [PMC]
2. Lenne P, Wawrezinieck L, Conchonaud F, Wurtz O, Boned A, Guo X, et al. Dynamic molecular confinement in the plasma membrane by microdomains and the cytoskeleton meshwork. EMBO J. 2006;25:3245–56. [DOI] [PubMed] [PMC]
3. Seelig A, Seelig J. The dynamic structure of fatty acyl chains in a phospholipid bilayer measured by deuterium magnetic resonance. Biochemistry. 1974;13:4839–45. [DOI] [PubMed]
4. McElhaney RN. The use of differential scanning calorimetry and differential thermal analysis in studies of model and biological membranes. Chem Phys Lipids. 1982;30:229–59. [DOI] [PubMed]
5. Sasaki Y, Suzuki Y, Yagi N, Adachi S, Ishibashi M, Suda H, et al. Tracking of individual nanocrystals using diffracted x rays. Phys Rev E Stat Phys Plasmas Fluids Relat Interdiscip Topics. 2000;62:3843–7. [DOI] [PubMed]
6. Sekiguchi H, Kuramochi M, Ikezaki K, Okamura Y, Yoshimura K, Matsubara K, et al. Diffracted X-ray Blinking Tracks Single Protein Motions. Sci Rep. 2018;8:17090. [DOI] [PubMed] [PMC]
7. Sasaki YC. Diffracted X-ray Tracking for Observing the Internal Motions of Individual Protein Molecules and Its Extended Methodologies. Int J Mol Sci. 2023;24:14829. [DOI] [PubMed] [PMC]
8. Fujimura S, Mio K, Kuramochi M, Sekiguchi H, Ikezaki K, Mio M, et al. Agonist and Antagonist-Diverted Twisting Motions of a Single TRPV1 Channel. J Phys Chem B. 2020;124:11617–24. [DOI] [PubMed]

9. Mio K, Ohkubo T, Sasaki D, Arai T, Sugiura M, Fujimura S, et al. Real-Time Observation of Capsaicin-Induced Intracellular Domain Dynamics of TRPV1 Using the Diffracted X-ray Tracking Method. Membranes (Basel). 2023;13:708. [DOI] [PubMed] [PMC]
10. Kuramochi M, Omata H, Ishihara M, Hanslin S, Mizumaki M, Kawamura N, et al. Tilting and rotational motions of silver halide crystal with diffracted X-ray blinking. Sci Rep. 2021;11:4097. [DOI] [PubMed] [PMC]
11. Chang J, Arai T, Kuramochi M, Inamasu R, Lee Z, Ohkubo T, et al. Dynamic observations of various oligomers in amyloid β isoforms using laboratory diffracted X-ray blinking. Biochem Biophys Rep. 2022;31:101298. [DOI] [PubMed] [PMC]
12. Inamasu R, Yamaguchi H, Arai T, Chang J, Kuramochi M, Mio K, et al. Observation of molecular motions in polymer thin films by laboratory grazing incidence diffracted X-ray blinking. Polym J. 2023;55:703–9. [DOI]
13. Shiina T, Ohkubo T, McGehee K, Inamasu R, Arai T, Sasaki D, et al. Real-Time Observation of Polymer Fluctuations During Phase Transition Using Transmission Electron Microscope. Polymers (Basel). 2025;17:292. [DOI] [PubMed] [PMC]
14. Chatzigeorgiou P, Mourelatou A, Pollatos E, Margari D, Zogzas N, Viras K, et al. Comparison of the thermal behavior and conformational changes in partially and fully hydrated dipalmitoylphosphatidylcholine systems. J Therm Anal Calorim. 2018;131:887–98. [DOI]
15. Kodama M, Kuwabara M, Seki S. Successive phase-transition phenomena and phase diagram of the phosphatidylcholine-water system as revealed by differential scanning calorimetry. Biochim Biophys Acta. 1982;689:567–70. [DOI]
16. Ulrich AS, Sami M, Watts A. Hydration of DOPC bilayers by differential scanning calorimetry. Biochim Biophys Acta. 1994;1191:225–30. [DOI] [PubMed]
17. Mabrey S, Sturtevant JM. Investigation of phase transitions of lipids and lipid mixtures by sensitivity differential scanning calorimetry. Proc Natl Acad Sci U S A. 1976;73:3862–6. [DOI] [PubMed] [PMC]
18. Owusu-Ware SK, Chowdhry BZ, Leharne SA, Antonijević MD. Phase behaviour of dehydrated phosphatidylcholines. J Therm Anal Calorim. 2017;127:415–21. [DOI]
19. Wu ES, Jacobson K, Papahadjopoulos D. Lateral diffusion in phospholipid multibilayers measured by fluorescence recovery after photobleaching. Biochemistry. 1977;16:3936–41. [DOI] [PubMed]
20. Cullis PR. Lateral diffusion rates of phosphatidylcholine in vesicle membranes: effects of cholesterol and hydrocarbon phase transitions. FEBS Lett. 1976;70:223–8. [DOI] [PubMed]
21. Lewis RN, Mak N, McElhaney RN. A differential scanning calorimetric study of the thermotropic phase behavior of model membranes composed of phosphatidylcholines containing linear saturated fatty acyl chains. Biochemistry. 1987;26:6118–26. [DOI] [PubMed]
22. Lewis RNAH, Zhang Y, McElhaney RN. Calorimetric and spectroscopic studies of the phase behavior and organization of lipid bilayer model membranes composed of binary mixtures of dimyristoylphosphatidylcholine and dimyristoylphosphatidylglycerol. Biochim Biophys Acta. 2005;1668:203–14. [DOI] [PubMed]
23. Fujiyoshi Y. Structural physiology based on electron crystallography. Protein Sci. 2011;20:806–17. [DOI] [PubMed] [PMC]
24. Grant T, Grigorieff N. Measuring the optimal exposure for single particle cryo-EM using a 2.6 Å reconstruction of rotavirus VP6. Elife. 2015;4:e06980. [DOI] [PubMed] [PMC]
25. Heimburg T. A model for the lipid pretransition: coupling of ripple formation with the chain-melting transition. Biophys J. 2000;78:1154–65. [DOI] [PubMed] [PMC]
26. Tonggu L, Wang L. Cryo-EM sample preparation method for extremely low concentration liposomes. Ultramicroscopy. 2020;208:112849. [DOI] [PubMed] [PMC]
27. Unwin N. Acetylcholine receptor channel imaged in the open state. Nature. 1995;373:37–43. [DOI] [PubMed]

28. Bhattacharjee S, Feng X, Maji S, Dadhwal P, Zhang Z, Brown ZP, et al. Time resolution in cryo-EM using a PDMS-based microfluidic chip assembly and its application to the study of HflX-mediated ribosome recycling. Cell. 2024;187:782–96.e23. [DOI] [PubMed] [PMC]
29. Burke SM, Avstrikova M, Noviello CM, Mukhtasimova N, Changeux J, Thakur GA, et al. Structural mechanisms of α7 nicotinic receptor allosteric modulation and activation. Cell. 2024;187: 1160–76.e21. [DOI] [PubMed] [PMC]
30. Papasergi-Scott MM, Pérez-Hernández G, Batebi H, Gao Y, Eskici G, Seven AB, et al. Time-resolved cryo-EM of G-protein activation by a GPCR. Nature. 2024;629:1182–91. [DOI] [PubMed] [PMC]
31. Koshino M, Tanaka T, Solin N, Suenaga K, Isobe H, Nakamura E. Imaging of single organic molecules in motion. Science. 2007;316:853. [DOI] [PubMed]
32. Harano K, Takenaga S, Okada S, Niimi Y, Yoshikai N, Isobe H, et al. Conformational analysis of single perfluoroalkyl chains by single-molecule real-time transmission electron microscopic imaging. J Am Chem Soc. 2014;136:466–73. [DOI] [PubMed]
33. Crowe JH, Crowe LM, Chapman D. Preservation of membranes in anhydrobiotic organisms: the role of trehalose. Science. 1984;223:701–3. [DOI] [PubMed]
34. Sakurai M, Furuki T, Akao K, Tanaka D, Nakahara Y, Kikawada T, et al. Vitrification is essential for anhydrobiosis in an African chironomid, Polypedilum vanderplanki. Proc Natl Acad Sci U S A. 2008; 105:5093–8. [DOI] [PubMed] [PMC]
35. Hoekstra FA, Golovina EA, Buitink J. Mechanisms of plant desiccation tolerance. Trends Plant Sci. 2001;6:431–8. [DOI] [PubMed]
36. Schäfer A, Salditt T, Rheinstädter MC. Atomic force microscopy study of thick lamellar stacks of phospholipid bilayers. Phys Rev E Stat Nonlin Soft Matter Phys. 2008;77:021905. [DOI] [PubMed]
37. Khandelia H, Duelund L, Pakkanen KI, Ipsen JH. Triglyceride blisters in lipid bilayers: implications for lipid droplet biogenesis and the mobile lipid signal in cancer cell membranes. PLoS One. 2010;5: e12811. [DOI] [PubMed] [PMC]